



Published in final edited form as:

Sci Transl Med. 2011 November 16; 3(109): 109ra116. doi:10.1126/scitranslmed.3003110.

Mathematical Model Identifies Blood Biomarker-Based Early Cancer Detection Strategies and Limitations

Sharon S. Hori¹ and Sanjiv S. Gambhir^{1,2,*}

¹Department of Radiology, Molecular Imaging Program at Stanford (MIPS), the Bio-X Program, Stanford University School of Medicine, Stanford, CA, USA

²Departments of Bioengineering and Materials Science & Engineering, Stanford University, Stanford, California, USA

Abstract

Most clinical blood biomarkers lack the necessary sensitivity and specificity to reliably detect cancer at an early stage, when it is best treatable. It is not yet clear how early a clinical blood assay can be used to detect cancer, or how biomarker-based strategies can be improved to enable earlier detection of smaller tumors. To address these issues, we developed a mathematical model describing dynamic plasma biomarker kinetics in relation to the growth of a tumor, beginning with a single cancer cell. To exemplify a realistic scenario in which biomarker is shed by both cancerous and non-cancerous cells, we primed the model on ovarian tumor growth and CA125 shedding data, for which tumor growth parameters and shedding rates are readily available in published literature. We found that a tumor could grow unnoticed for over 10.1 years and reach a volume of (20.44 mm)³ before becoming detectable by current clinical blood assays. Model parameters were perturbed over log-orders of magnitude to quantify ideal shedding rates and identify other blood-based strategies required for early sub-millimeter tumor detectability. Detection times we estimated are consistent with recently published tumor progression timelines based on clinical genomic sequencing data for several cancers. In this study, we rigorously showed that shedding rates of current clinical blood biomarkers are likely 10⁴-fold too low to enable detection of a developing tumor within the first decade of tumor growth. The model presented here can be extended to virtually any solid cancer and associated biomarkers.

*To whom correspondence should be addressed. Molecular Imaging Program at Stanford, Departments of Radiology and Bioengineering, Clark Center E150, 318 Campus Drive, Stanford, CA 94305-5427, USA. sgambhir@stanford.edu.

LIST OF SUPPLEMENTARY MATERIAL

Derivation of Model Equations.

Supplementary Methods.

Extension of Model to Include Benign Growths.

Discussion of Five Example Early Detection Strategies.

Supplementary Sensitivity Analyses.

Fig. S1. Earliest possible detection time vs. actual blood-based detection time.

Fig. S2. Earliest possible detection time and tumor diameter at detection, assuming biomarker shedding by tumor cells only.

Fig. S3. Earliest possible detection time and tumor diameter at detection, assuming biomarker shedding by tumor and healthy cells.

Fig. S4. One-way sensitivity analysis: tumor diameter vs. p .

Fig. S5. Two-way sensitivity analyses assuming mono-exponential tumor growth and biomarker shedding by tumor cells only.

Fig. S6. Two-way sensitivity analyses assuming mono-exponential tumor growth and biomarker shedding by tumor and healthy cells.

Fig. S7. Two-way sensitivity analyses assuming Gompertzian tumor growth and biomarker shedding by tumor cells only.

Fig. S8. Two-way sensitivity analyses assuming Gompertzian tumor growth and biomarker shedding by tumor and healthy cells.

References.

Author contributions: S.S.H. and S.S.G. designed the mathematical model and study. S.S.H. implemented the mathematical model and collected data for the study. S.S.H. and S.S.G. analyzed the data and contributed to the writing of the manuscript.

Competing Interests: The authors declare that they have no competing financial interests.

INTRODUCTION

Most cancers can be more effectively treated if they are discovered early, when the tumor is confined to its primary site (1, 2). In these early stages, surgical resection and conventional treatments are often curative. For example, ovarian cancer patients diagnosed at Stage I exhibit 5-year survival rates as high as 90%; however, over 80% of ovarian cancer patients are diagnosed when symptoms arise during Stages III and IV, when 5-year survival rates become less than 30% (3, 4). Approaches to detect ovarian cancer in its earliest stages, when the cancer is still confined to the ovary, may best help reduce mortality. However, current screening methods for ovarian and other cancers are still inadequate due to lack of test sensitivity and specificity (3, 4).

Early detection efforts have focused on developing screening assays to monitor levels of cancer blood biomarkers – proteins, methylated DNA or other signatures of cancer that are “shed” (secreted or released) into blood (2, 5, 6). Tumor-specific microRNAs have been highlighted as ideal candidates for blood-based early cancer detection due to their tissue-specific dysregulated expression in cancer, high abundance and stability in blood, and sensitive methods such as qRT-PCR readily available for quantification (7–10). It is hoped that cancer blood biomarkers will have the potential to accurately diagnose disease, monitor treatment, and provide a reliable screening method that also reduces health-care expenses resulting from late-stage treatment regimens (1, 2, 6). Unfortunately, of the thousands of potential biomarkers reported and examined for diagnostic use, only few are routinely being used in the clinic, and many (if not most) are of limited utility in detecting “relevant” cancers (fast-growing cancers that will likely become lethal, thereby requiring immediate intervention) at an early or curable stage (2). The lack of early cancer biomarkers is currently a major obstacle for blood-based early detection. Development of reliable blood assays with effective biomarkers, followed by sensitive molecular imaging exams to verify the blood test findings as well as determine the stage of disease and localize tumor burden, would expedite diagnosis and thereby accelerate the treatment process (2).

It is still unclear whether biomarkers released by small tumors ($< 10 \text{ mm}^3$) are capable of being detected in blood. One reason is that several biological factors involved in early tumor biomarker shedding (e.g., secretion rates from tumor and healthy cell populations, the amount of biomarker entering tumor vessels from the interstitium, the effects of cancer heterogeneity on tumor growth and biomarker shedding rates, etc.) have not been quantitatively assessed *in vivo*. Thus, the correlation between blood biomarker levels and tumor volume (or tumor growth) is not well understood. A separate issue is the ability of blood biomarker assays to correctly identify cancer in a large patient population. Since healthy (non-cancerous) cells may also shed the same biomarker, at varying levels among individuals of a population, there is a probability that a healthy cancer-free patient will have abnormally high levels of blood biomarker. This contributes to low test specificity, i.e., a higher number of assay false positives.

To address these issues, our laboratory recently developed the first mathematical model to determine the smallest tumor volume likely detectable by current blood-based biomarker assays for ovarian and prostate cancers (11). However, this simple modeling study was performed assuming steady state, i.e., at a specific time when biomarker fluxes into and out of plasma are assumed equal. These steady state assumptions generally hold only in the special circumstance of a non-growing tumor population. A more realistic model incorporating *dynamic* (changing) biomarker levels in blood over time (due to an increase or decrease in the number of cancer cells), as would be expected during tumor growth and treatment, would clearly be more relevant. No mathematical models have since been

developed that can be used to monitor fluctuating blood biomarker levels in relation to a growing tumor.

Incorporating time-dependency into the biomarker secretion model is an important and necessary next-step in evaluating blood biomarker early detection capabilities because it allows us to: 1) determine the minimum period of time a *growing* tumor cell population would need to proliferate before being detectable by blood-based assays, and 2) identify biomarker-associated parameters that significantly affect early detection capability, and quantify how much these parameters would need to be manipulated to improve detection by blood-based assays. We addressed these issues here, by incorporating tumor growth into a new linear 1-compartment biomarker secretion model, to assess *dynamic* plasma biomarker kinetics in relation to the genesis of cancer, beginning with a single parental tumor cell. We aimed to quantify the time required for a growing malignant tumor cell population to reach a sufficient size so that its shed blood biomarker levels were high enough to be detected using current clinical blood biomarker assays, and then we used the model to calculate changes in detection capabilities based on log-order perturbations in fundamental parameters for biomarker shedding. Importantly, the model can be used to help identify the biomarker-related parameters that most greatly impact blood-based early cancer detection, and quantify how far each baseline parameter value would need to change in order to achieve earlier (sub-millimeter) tumor detection.

RESULTS

Development of a mathematical model of plasma biomarker kinetics

A biomarker in whole-body plasma is assumed to be well-mixed and homogenous, and therefore can be described using 1-compartment model kinetics (Fig. 1). Although biomarker may be shed from benign and malignant tumors, we focus here on biomarker shed from malignant cells only, as blood detection would then consequently reflect the presence of a relevant cancer. As benign tumors may be detectable before they give rise to malignant subclones, alternative equations for benign tumor shedding are presented in the Supplementary Material (see “Extension of Model to Include Benign Growths”).

Plasma biomarker influx is the sum of biomarker shedding from tumor cells, $u_T(t)$, and from healthy cells, $u_H(t)$. Each influx is a function of: 1) the fraction of shed biomarker entering tumor vasculature, $f_{P_{L,T}}$, or healthy vasculature, $f_{P_{L,H}}$, which may differ due to the abnormal leakiness and dilation of tumor blood vessels (12) and the extent of biomarker degradation in the tumor microenvironment; 2) the shedding rates of biomarker from tumor cells, R_T , or healthy cells, R_H , both of which are assumed constant; and 3) the number of tumor cells, $N_T(t)$, or healthy cells, $N_H(t)$, shedding biomarker at a given time t . Note that if a biomarker is exclusively shed by cancer stem cells, then $N_T(t)$ may represent a minority population of cancer stem cells present in the growing tumor.

In this study, the process of “biomarker shedding” is loosely defined as the addition of biomarker into the interstitium by any biological mechanism, e.g., the secretory pathway or the release of cellular degradation products following apoptosis or necrosis (13, 14). Assuming that all tumor cells shed biomarker, and that the biomarker shedding rates are constant (but possibly different) for tumor and healthy cells, we attribute the increase in plasma biomarker levels to the growth of the biomarker-shedding tumor cell population (tumor burden), which includes all primary and metastatic tumor cells, if any. The number of tumor cells, $N_T(t)$, is modeled using the Gompertzian function (15, 16),

$$N_T(t) = N_{T,0} e^{\frac{k_{GR}}{k_{decay}} (1 - e^{-k_{decay}t})},$$

where $N_{T,0}$ is the number of tumor cells present at time $t = 0$, k_{GR} is the fractional growth rate of the tumor population (day^{-1}), and k_{decay} is the decaying rate of tumor growth (day^{-1}). Note that k_{GR} is related to tumor doubling time (t_{DT}) according to the equation $k_{GR} = (\ln 2)/t_{DT}$. As $k_{decay} \rightarrow \infty$, the number of tumor cells more quickly approaches its maximum size. As $k_{decay} \rightarrow 0$, the Gompertzian function simplifies to the mono-exponential growth function,

$$N_T(t) = N_{T,0} e^{k_{GR}t}.$$

We note that while such simplistic, unbounded, strictly increasing growth models may not fully encapsulate the heterogeneity of cancer (in terms of varying degrees of cell proliferation, necrosis, angiogenesis, biomarker shedding rates, etc., in different regions of the tumor) as some multi-scale models may, they are sufficient for calculating *earliest* possible detection times. We simulated tumor growth from $t = 0$ days, which can be interpreted as the time of tumor onset (or “genesis” of a tumor), at which a premalignant cell transforms into the first malignant (tumor) cell capable of shedding the biomarker(s) of interest.

In this study, a “healthy cell” is defined to be any non-cancerous cell in any organ of the body that sheds the same biomarker as tumor cells (possibly at a different rate, R_H). Unlike the growing tumor cell population, the number of healthy cells is assumed constant, i.e., the rates of healthy cell growth and death are assumed equal. Therefore $N_H(t) = N_{H,0}$, where $N_{H,0}$ is the number of healthy biomarker-shedding cells.

Biomarker elimination from plasma may occur via a number of processes, including irreversible excretion in kidneys, degradation in liver, or breakdown by proteases. The rate of plasma biomarker elimination (k_{EL}) is assumed linear, i.e., a fraction of total biomarker in plasma is irreversibly removed per unit time. We calculated k_{EL} based on the half-life $t_{1/2}$ of biomarker in blood, where $k_{EL} = (\ln 2)/t_{1/2}$.

It is important to note that the general model structure described here is used to determine the earliest possible detection time for a tumor, by supposing a continuous and strictly increasing tumor growth model and constant biomarker secretion. A more realistic depiction of biomarker blood levels and actual detection times can be developed in the future by incorporating more complex (multi-scale) growth and secretion models, as these mechanisms become better studied, and as the relevant clinical data becomes available.

Example: Ovarian Cancer and CA125 Secretion

The 1-compartment model presented here is generalizable for any solid cancer and corresponding shed biomarker(s). To exemplify a realistic scenario in which biomarker is shed by both tumor and healthy cells, we used parameter values based on ovarian carcinoma growth and associated CA125 shedding, which have been well-studied with all parameter values available in published literature (11, 17–27) (Tables 1 and 2). We note that the number of detectable blood biomarker proteins/molecules can be easily calculated for biomarkers measured in mass units (e.g., ng). However, this conversion is not possible here because CA125 is measured in arbitrary units (U).

To date, there is no single biomarker capable of detecting any relevant early stage cancer with adequate sensitivity and specificity. It should be noted that while CA125 is widely used to monitor ovarian cancer recurrence, it is not praised as an early detection biomarker, as it lacks sensitivity in screening asymptomatic patients, and has a high rate of false positives due to its elevated presence in many non-cancerous cases (menstruation and pregnancy, endometriosis, uterine fibroids, liver cirrhosis) as well as non-ovarian cancers (pancreatic, breast, bladder, lung, liver) (28, 29). We used CA125 as an example in the current work not because it will necessarily prove useful for detecting early ovarian cancer, but because it has been sufficiently studied with all required model parameter values available in literature. Although many new blood biomarkers have been discovered in the past 10 years (for ovarian and other cancers), few have been widely tested for screening purposes (3, 4, 6), let alone studied adequately enough to provide the parameter values needed for the current study.

Therefore, the ovarian cancer growth and CA125 shedding literature values were used here to provide realistic baseline values for model simulations, and were then examined over several log-orders of magnitude in subsequent sensitivity analyses. These results were compared against published estimates of tumor progression timelines for other cancers.

Assessing performance of current clinical biomarker assays

In this study, the model was used to examine two cases: 1) biomarker shedding by tumor cells only; and 2) biomarker shedding by tumor and healthy cells (Fig. S1). The first case is ideal for the early cancer detection setting because any biomarker detected in blood can be attributed to the presence of at least one cancer cell. In the second case, additional secretion by healthy cells induces an inherent background signal that will also confound biomarker levels indicative of the presence of a tumor.

When a biomarker is not shed by healthy cells, the number of tumor cells detectable is strictly dependent on the sensitivity of the blood assay. An assay with a lower detection limit will therefore be able to detect fewer tumor cells. Assuming a baseline detection limit of $d = 1.5$ U/ml (the detection limit of current clinical CA125 ELISA assays) and all other baseline parameters indicated in Tables 1 and 2, the model indicates that 1.22×10^8 tumor cells are detectable, corresponding to a tumor volume of $(8.48 \text{ mm})^3$ (Fig. S2A–G, dashed vertical lines). This is potentially a 5-fold improvement over the mean tumor volume $((42 \text{ mm})^3)$ detected using ultrasound at clinical diagnosis (30). Approximately 8.8 years (assuming mono-exponential growth) to 10.6 years (assuming Gompertzian growth) are required for the tumor to reach a volume of $(8.48 \text{ mm})^3$ from the genesis of the first cancer cell. This detectable tumor burden includes all biomarker-shedding primary and metastatic (if any) tumor cells.

Assuming additional shedding of biomarker by healthy cells, the ability to detect a growing tumor is no longer dependent on the sensitivity of the biomarker assay alone, since healthy patients will presumably be shedding detectable levels of biomarker. The question then becomes, how much of the plasma biomarker is attributed to tumor cells? For CA125, the mean concentration in healthy women is 13.1 U/ml (22), with an estimated 99.9% having less than 34.11 U/ml (11). We found that a growing tumor must reach 1.71×10^9 cells or $(20.44 \text{ mm})^3$ to shed enough CA125 to exceed this healthy-state cut-off limit (Fig. S3A–H, dashed vertical lines). This would require 10.1 years (assuming mono-exponential growth) to 12.6 years (assuming Gompertzian growth) after the genesis of the initial tumor cell.

Simulated Strategies for Earlier Cancer Detection

The baseline parameter values used in the model provided ranges of minimum detection time nearing one decade (8.8 to 10.1 years) and minimum tumor burden well exceeding (1 mm^3 volume ($(8.48 \text{ mm})^3$ to $(20.44 \text{ mm})^3$). We next sought to determine the magnitude the shedding-related ($f_{\text{PL,T}}$, R_{T} , k_{EL} and $f_{\text{PL,H}}R_{\text{H}}N_{\text{H,0}}$) and assay-related (d) parameters would need to increase or decrease to provide earlier detection times (i.e., smaller tumor volumes). To do this, we systematically calculated the value each parameter would need to be to achieve a volume that was 10-fold, 100-fold, ..., 10^9 -fold lower than the baseline minimum tumor burden volume. We excluded tumor growth and disease cut-off parameters from these sensitivity analyses, as direct parameter manipulations to decrease tumor volume or lower the healthy-disease threshold would only artificially decrease early detection time. (Effects of perturbations in these parameter values, however, are shown in Fig. S2 and S3).

Table 3 provides results for the case of biomarker shedding by tumor cells only. A 10-fold increase in tumor cell shedding rate R_{T} , or a 10-fold decrease in assay detection limit d , could allow a $(3.94 \text{ mm})^3$ tumor to be detectable within 7.7 years after its genesis. Although there are currently no known biomarkers with such high shedding rates, or clinical assays with such good sensitivities, these values suggest that when healthy cell biomarker shedding is not involved, better blood-based detection strategies might include identification of other biomarkers that are shed in higher amounts, as well as the development of more sensitive technologies to detect lower levels of biomarker in blood. These strategies are not unreasonable. The ability to increase tumor biomarker secretion rates up to 4-fold is now becoming possible, with emerging strategies such as the application of high frequency ultrasound to induce shedding from suspect tumor sites (31). Furthermore, newer detection technologies are now capable of detecting biomarker concentrations as low as 50 attomolar ($5 \times 10^{-17} \text{ M}$) (32, 33).

Smaller tumor volumes and earlier detection times for other hypothetical parameter scenarios are indicated in Table 3 and described in the Supplementary Material (see “Discussion of Five Example Early Detection Strategies”). Interestingly, tumor volumes smaller than $(3.94 \text{ mm})^3$ are not detectable by altering $f_{\text{PL,T}}$ or k_{EL} alone, as this would require physiologically implausible parameter values, i.e., $f_{\text{PL,T}} > 1$ or $k_{\text{EL}} < 0$.

Table 4 indicates results for the case of biomarker shedding by tumor and healthy cells. In this case, the model predicts that a 13-month improvement in early detection time (from 10.1 yr to 9.0 yr) may be possible if tumor shedding rate R_{T} were 10-fold higher, or if healthy cell shedding $f_{\text{PL,H}}R_{\text{H}}N_{\text{H,0}}$ were 10-fold lower. Decreasing $f_{\text{PL,H}}R_{\text{H}}N_{\text{H,0}}$ corresponds to using biomarkers that have lower average levels in the healthy cancer-free population (e.g., for CA125, a 10-fold decrease in baseline $f_{\text{PL,H}}R_{\text{H}}N_{\text{H,0}}$ would correspond to an average biomarker concentration of 1.3 U/ml in the healthy population). Note that k_{EL} is not listed in Table 4, as the detectable tumor volume does not decrease even as k_{EL} is altered (Fig. S3F).

As CA125 may not be the ideal biomarker for early detection, we next used the model to explore the characteristics of an ideal candidate biomarker by simulating the following scenarios: increasing vascular permeability to 100% ($f_{\text{PL,T}} = 1$), eliminating healthy cell biomarker shedding, increasing tumor cell biomarker shedding, and decreasing assay detection limit. Fig. 2 summarizes some specific strategies for detecting a tumor at an earlier stage, based on data from Tables 3 and 4 and Fig. S2 and S3. Point A indicates the current status of clinical ELISA assays for measuring a biomarker shed by both tumor and healthy cells (10.1 yr, $(20.44 \text{ mm})^3$). Performance is only slightly improved if 100% of shed biomarker reaches plasma (Point B, 9.0 yr, $(9.49 \text{ mm})^3$), or if there is no background shedding by healthy cells (Point C, 8.8 yr, $(8.48 \text{ mm})^3$). Assaying for biomarkers that are

shed from tumor cells at 10^3 -fold higher shedding rates (despite baseline values for background healthy cell shedding) may allow detection of tumors as low as 2-mm in diameter (Point D, 6.8 yr, $(2.04 \text{ mm})^3$). Improvements in assay sensitivity will only allow sub-millimeter tumor detectability when healthy cell biomarker shedding is essentially negligible relative to tumor cell shedding; even then, at least a 10^3 -fold improvement in the assay detection limit is required (Point E, 5.6 yr, $(0.85 \text{ mm})^3$; Point F, 3.4 yr, $(0.18 \text{ mm})^3$). In these optimal scenarios, sub-millimeter tumor detection may occur at least 4.5 years earlier relative to baseline (10.1 yr), reducing early detection time by 45%. Note that if a biomarker were shed by tumor cells only, and assay detection limits remained at baseline 1.5 U/ml, the model indicates that Points E and F could also be achieved by increasing tumor cell shedding rate 10^3 -fold and 10^5 -fold respectively (Table 3).

We note that n -way sensitivity analyses can be conducted to simultaneously examine how the model outputs would be affected by simultaneous perturbations in multiple parameter values. Examples of two-way sensitivity analyses are shown in Fig. S5–S8.

DISCUSSION

“Early” relevant cancer detection is only effective if an early-stage tumor can be detected when the cancer is still treatable. In the current study, we used a mathematical framework to evaluate the early cancer detection problem, to motivate design of new experiments that challenge current hypotheses regarding biomarker detectability, and to determine, by rigorous sensitivity analyses, whether blood detection of single cancer biomarkers can ever become a feasible end-all strategy for diagnosing early-stage cancers.

Based on published ovarian carcinoma growth and CA125 shedding parameters (Tables 1 and 2), we found that “early” detection of a continuously growing tumor burden using currently available assays may require at least 8.8 to 10.1 years following the appearance of the first cancer cell (Tables 3 and 4). These early detection times, which are dependent on the extent of healthy cell biomarker shedding, are still only optimistic lower limit estimates of time until detection because they were calculated assuming (unbounded and strictly increasing) mono-exponential growth. To account for the possibility that the rate of tumor growth may decrease as tumor volume increases, we also used a Gompertzian growth model to estimate time until detection, and found that a tumor may grow for 10.6 to 12.6 years (Fig. S2 and S3, baseline dashed lines) before being detectable by current clinical ELISA assays. In addition, early-stage microscopic tumors likely undergo an occult dormancy period in which initial tumor growth remains static and limited, possibly because vasculature may not yet be fully established (which may also limit biomarker influx into blood) (34, 35). Thus, it would not be unreasonable to assume that these cancers may go undetected for several years longer.

Interestingly, these model predictions are consistent with published cancer progression timelines recently reported for other human cancers (36–39). Yachida and colleagues analyzed genomic sequencing data of metastases from seven patients with Stage IV pancreatic cancer and calculated that the first parental (non-metastatic) founder cancer cell may require 6.8 years to generate subclones with metastatic potential; these subclones could give rise to distant metastases within 2.7 years, with clinical diagnosis likely occurring 18–20 years after the genesis of the founder cell (38). Jones and colleagues found that a benign colorectal tumor might require 17 years to develop into an advanced carcinoma (36). On a larger timescale, Meza and colleagues reported that the average time from an initial premalignant mutation to the ultimate conversion of a detectable cancer (based on no-extinction and in the absence of censoring due to other causes of death) in pancreatic and colorectal cancers may take 50 years (39). While tumor progression timelines may vary for

different cancers, these studies share in common the implications that there exists at least a period of 7–10 years before a primary tumor begins to metastasize. The model presented here indicates that the cancer biomarkers and blood assays currently being used in clinic may not be capable of detecting a growing tumor burden until metastasis has likely occurred.

Here, we pinpoint where blood biomarker assays enter on the timeline of tumor growth. The baseline parameter values used in this simulation-based analysis provide a reference point for how well current assays are performing and how future ones will have to perform to likely be useful. Since the “age” of a tumor cannot be accurately measured at clinical diagnosis, we were unable to compare the model predictions directly to relevant patient data. Direct extrapolation of the model predictions to the clinic is particularly difficult to validate at this time; there is currently no available patient data correlating tumor size with plasma biomarker levels, before and after cancer diagnosis, for multiple time points in the same subject, throughout the natural course of disease progression. When relevant cancers are discovered early, they are typically not serially monitored for both blood biomarker levels and tumor volumes without treatment or intervention, and therefore we could not compare these results to clinical data for increasing biomarker levels and tumor growth for large patient populations.

It is not surprising that the relationship between tumor size and blood biomarker levels is not entirely straightforward or well understood. Biomarker shedding is likely dependent on many complex nonlinear processes, e.g., vascularization and tumor growth, and these processes likely influence each other. However, several studies have shown that serum CA125 levels may reflect tumor burden, as well as therapeutic response, in many epithelial ovarian cancers (11, 17, 40–42). One study found that elevated CA125 levels (>35 U/ml) were present only when ovarian tumor size was greater than 10 cm (43). More recently, it has been shown that CA125 levels were significantly higher in female patients with malignant ovarian tumors versus benign masses ($p < 0.001$) (30).

It should be noted that the model’s predictive capability is limited by the model assumptions and available data. First, the model does not include circadian variations in biomarker shedding, as may be expected in tumors or other organs, since these fluctuations have not been adequately studied to date. Here, we used constant shedding rates obtained from published cell culture experiments, which specifically account for the cumulative amount of biomarker shed per cell in a 48-hr period (27). To our knowledge, there is no *in vivo* information available in literature regarding the time-varying amount of biomarker shed per cell (cancerous or non-cancerous) in living tumor-bearing animals or in patients with any cancer. It should be noted, however, that nonlinear shedding rates can easily be incorporated into future generations of the model (e.g., using a time-dependent function $R_T(t)$). Second, the tumor burden volume reported here represents the total number of biomarker-shedding primary and metastatic cells. The model does not account for different shedding rates or growth rates in primary and metastatic tumor cell populations, as these differences, to our knowledge, have not been measured *in vivo*. It should also be noted that the goal of this study (and more generally, of the early cancer detection problem) is not to detect advanced cancers that have already metastasized, but rather to detect the primary tumor before any significant metastasis has occurred. Therefore, while the mono-exponential and Gompertzian growth models may not hold for advanced stage cancers involving more complex tumor processes (such as metastasis, which may require more than 18 years following the genesis of the parental tumor cell (38)), they are likely sufficient for studying the early growth a small primary tumor. Finally, we do not model the fraction of biomarker entering blood as a time-varying fraction, as this time-dependency has not been reported and is not easily generalizable. It is expected that the amount of biomarker entering blood may

change with respect to tumor size, angiogenesis and necrosis. Interestingly, this fraction may now be better studied in small animal models *in vivo* using intravital microscopy (44) to monitor the intratumoral distribution of fluorescent secretable biomarkers such as SEGF (45) in tumor-bearing animals.

New biomarkers are constantly being discovered and each will need to be systematically and rigorously evaluated for its potential to distinguish between healthy and early cancer states. In addition, it is becoming clear that a single biomarker alone may not be capable of detecting cancer with sufficient sensitivity and specificity; instead, panels of up to 10 biomarkers may be needed (29, 46). The mathematical model presented here can be extended to virtually any solid cancer and corresponding biomarker panel shed, assuming that such parameter values are available or can be measured. Importantly, this model is not limited to proteins, but can be applied to a diverse spectrum of secreted biomarkers. For example, hundreds of miRNAs have now been detected in blood at trace levels, using PCR and bead-based hybridization methods (47). The time course and characteristics of tumor growth can potentially be evaluated using this mathematical framework by analyzing hundreds of miRNA profiles simultaneously.

The one-way sensitivity analyses performed in this study are a logical “next-step” in the current predicament in which relevant clinical data is lacking; we can observe how the model outputs (early detection time and tumor volume) respond to perturbations in the parameter values, without focusing on the absolute values of the parameters themselves. The model is not only used to estimate the minimum “age” of a tumor at blood-based clinical diagnosis; a more powerful result is the identification of parameters that may be capable (or incapable) of accelerating early cancer detection, and more importantly, quantifying how far these parameters must be perturbed in order to achieve *earlier* (sub-millimeter) detection. The estimated 10-year period until detection, as determined in the likely case when both tumor and healthy cells shed the same assayed biomarker, indicates that there is still time for earlier blood-based detection. This may become possible as the time-varying or nonlinear biological complexities of biomarker shedding, angiogenesis, tumor dormancy and tumor growth become better understood.

MATERIALS AND METHODS

Calculating Time Until Detection and Corresponding Tumor Volume

The change in the amount (mass) of plasma biomarker with respect to time is equal to the difference between the influx of biomarker into plasma, as shed by tumor cells and healthy cells, $u_T(t) + u_H(t)$, and the outflux of biomarker from plasma, $k_{EL}q_{PL}(t)$. Plasma biomarker mass was converted to units of concentration by dividing by V_{PL} , the mean plasma volume of a 70-kg female (Table 1).

For the case of biomarker shedding by tumor cells only, the earliest possible detection time (t_D) was calculated by setting plasma biomarker concentration $q_{PL}(t)/V_{PL}$ equal to d , the detection limit of the assay, and subsequently solving for t . The corresponding number of tumor cells was then calculated by substituting t_D into either the Gompertzian or mono-exponential growth function.

For the case of biomarker shedding by tumor and healthy cells, values of t_D and the corresponding number of tumor cells at detection were calculated similarly, except plasma biomarker concentration $q_{PL}(t)/V_{PL}$ was set equal to c , the plasma biomarker “cut-off” level for healthy and disease states. It should be noted that patients with biomarker levels $q_{PL}(t) < c$ would be categorized as disease-negative, whereas patients with biomarker levels $q_{PL}(t) > c$ would be classified as disease-positive. The cut-off level c was calculated previously (11),

and was based on the mean biomarker level in healthy patients, which was assumed to represent a steady-state mass of plasma biomarker,

$$q_{ss} = \frac{f_{PL,H} R_H N_{H,0}}{k_{EL}}$$

The number of detectable tumor cells was converted to tumor volume using two assumptions: 1) Tumor cells comprise $p = 20\%$ of the total tumor volume (11); and 2) the tumor has a cell density of 1×10^6 cells/mm³ (11, 19). These assumptions were made to help the reader interpret the estimated tumor size, not to provide a literal prediction of clinical tumor volume. The value of p was chosen as a lower limit (11, 20) and its impact on the calculation of tumor volume is illustrated in Fig. S4–S8 (see also “Supplementary Sensitivity Analyses”). In this study, tumor volume was described in terms of tumor “diameter,” where $volume = (diameter)^3$.

Sensitivity Analyses Performed

We first calculated t_D and the corresponding tumor diameter assuming baseline parameter values (Table 2) and either a Gompertzian or mono-exponential tumor growth model. We then performed one-way sensitivity analyses on the 9 parameters listed in Table 2, with parameter values and ranges justified in the Supplementary Methods. Specifically, for a given parameter, we divided the “range simulated” into 21 subintervals using equally spaced nodes, and calculated new t_D and tumor diameter values at each node. All calculations were performed using Mathematica 6.0 (Wolfram Research).

Identifying Strategies to Improve Early Detection

To identify the model parameters most capable of affecting t_D and tumor diameter, we systematically calculated the value each parameter would need to be to achieve a tumor volume 10-fold, 100-fold, ..., or 10^9 -fold lower than the baseline minimum tumor volume. Non-physiological parameter values were declared infeasible. See also “Discussion of Five Example Early Detection Strategies” in the Supplementary Material.

Supplementary Material

Refer to Web version on PubMed Central for supplementary material.

Acknowledgments

We thank Sarah Hawley and Jason Thorpe for their helpful discussions; Daniela Starcevic, Sarah Hawley, Nicholas Hughes, John Ronald, Bryan Smith and Laura Sasportas for their critical reading of the manuscript; Jim Strommer for his assistance with the manuscript figures.

Funding: Supported in part by the Canary Foundation and NIH grants NCI ICMIC P50 CA114747 and NCI U01 EDNRN CA152737 to S.S.G., and NIH R25T CA118681 to S.S.H.

REFERENCES

1. Etzioni R, Urban N, Ramsey S, McIntosh M, Schwartz S, Reid B, Radich J, Anderson G, Hartwell L. The case for early detection. *Nat Rev Cancer*. 2003; 3:243–252. [PubMed: 12671663]
2. Gambhir SS. Novel Strategies and Challenges for Early Relevant Cancer Detection. *Science*. 2011 In Press.
3. Das PM, Bast RC Jr. Early detection of ovarian cancer. *Biomark Med*. 2008; 2:291–303. [PubMed: 20477415]

4. Dutta S, Wang FQ, Fishman DA. The dire need to develop a clinically validated screening method for the detection of early-stage ovarian cancer. *Biomark Med.* 2010; 4:437–439. [PubMed: 20550476]
5. Tainsky MA. Genomic and proteomic biomarkers for cancer: a multitude of opportunities. *Biochim Biophys Acta.* 2009; 1796:176–193. [PubMed: 19406210]
6. Poste G. Bring on the biomarkers. *Nature.* 2011; 469:156–157. [PubMed: 21228852]
7. Kroh EM, Parkin RK, Mitchell PS, Tewari M. Analysis of circulating microRNA biomarkers in plasma and serum using quantitative reverse transcription-PCR (qRT-PCR). *Methods.* 2010; 50:298–301. [PubMed: 20146939]
8. Mitchell PS, Parkin RK, Kroh EM, Fritz BR, Wyman SK, Pogosova-Agadjanian EL, Peterson A, Noteboom J, O'Briant KC, Allen A, Lin DW, Urban N, Drescher CW, Knudsen BS, Stirewalt DL, Gentleman R, Vessella RL, Nelson PS, Martin DB, Tewari M. Circulating microRNAs as stable blood-based markers for cancer detection. *Proc Natl Acad Sci U S A.* 2008; 105:10513–10518. [PubMed: 18663219]
9. Cummins JM, He Y, Leary RJ, Pagliarini R, Diaz LA Jr, Sjoblom T, Barad O, Bentwich Z, Szafranska AE, Labourier E, Raymond CK, Roberts BS, Juhl H, Kinzler KW, Vogelstein B, Velculescu VE. The colorectal microRNAome. *Proc Natl Acad Sci U S A.* 2006; 103:3687–3692. [PubMed: 16505370]
10. Grady WM, Tewari M. The next thing in prognostic molecular markers: microRNA signatures of cancer. *Gut.* 2010; 59:706–708. [PubMed: 20551450]
11. Lutz AM, Willmann JK, Cochran FV, Ray P, Gambhir SS. Cancer screening: a mathematical model relating secreted blood biomarker levels to tumor sizes. *PLoS Med.* 2008; 5:e170. [PubMed: 18715113]
12. Jain RK. Normalization of tumor vasculature: an emerging concept in antiangiogenic therapy. *Science.* 2005; 307:58–62. [PubMed: 15637262]
13. Kulasingam V, Diamandis EP. Strategies for discovering novel cancer biomarkers through utilization of emerging technologies. *Nat Clin Pract Oncol.* 2008; 5:588–599. [PubMed: 18695711]
14. Petricoin EF, Belluco C, Araujo RP, Liotta LA. The blood peptidome: a higher dimension of information content for cancer biomarker discovery. *Nat Rev Cancer.* 2006; 6:961–967. [PubMed: 17093504]
15. Laird AK. Dynamics of Tumour Growth: Comparison of Growth Rates and Extrapolation of Growth Curve to One Cell. *Br J Cancer.* 1965; 19:278–291. [PubMed: 14316202]
16. Norton L, Simon R, Brereton HD, Bogden AE. Predicting the course of Gompertzian growth. *Nature.* 1976; 264:542–545. [PubMed: 1004590]
17. Bast RC Jr, Klug TL, St John E, Jenison E, Niloff JM, Lazarus H, Berkowitz RS, Leavitt T, Griffiths CT, Parker L, Zurawski VR Jr, Knapp RC. A radioimmunoassay using a monoclonal antibody to monitor the course of epithelial ovarian cancer. *N Engl J Med.* 1983; 309:883–887. [PubMed: 6310399]
18. Brown PO, Palmer C. The preclinical natural history of serous ovarian cancer: defining the target for early detection. *PLoS Med.* 2009; 6:e1000114. [PubMed: 19636370]
19. Enderle, JD.; Blanchard, SM.; Bronzino, JD. Academic Press series in biomedical engineering. ed. 2nd. Boston: Elsevier Academic Press, Amsterdam; 2005. Introduction to biomedical engineering. pp. xxi, 1118 p.
20. Gullino PM, Grantham FH, Smith SH. The Interstitial Water Space of Tumors. *Cancer Res.* 1965; 25:727–731. [PubMed: 14347560]
21. Kenemans P, van Kamp GJ, Oehr P, Verstraeten RA. Heterologous double-determinant immunoradiometric assay CA 125 II: reliable second-generation immunoassay for determining CA 125 in serum. *Clin Chem.* 1993; 39:2509–2513. [PubMed: 8252723]
22. Klug TL, Bast RC Jr, Niloff JM, Knapp RC, Zurawski VR Jr. Monoclonal antibody immunoradiometric assay for an antigenic determinant (CA 125) associated with human epithelial ovarian carcinomas. *Cancer Res.* 1984; 44:1048–1053. [PubMed: 6198078]

23. Mastropaolo W, Fernandez Z, Miller EL. Pronounced increases in the concentration of an ovarian tumor marker, CA-125, in serum of a healthy subject during menstruation. *Clin Chem*. 1986; 32:2110–2111. [PubMed: 3465487]
24. Mongia SK, Rawlins ML, Owen WE, Roberts WL. Performance characteristics of seven automated CA 125 assays. *Am J Clin Pathol*. 2006; 125:921–927. [PubMed: 16690492]
25. Sok D, Clarizia LJ, Farris LR, McDonald MJ. Novel fluoroimmunoassay for ovarian cancer biomarker CA-125. *Anal Bioanal Chem*. 2009; 393:1521–1523. [PubMed: 19145430]
26. Warrell, DA. *Oxford textbook of medicine*. ed. 4th. Oxford ; New York: Oxford University Press; 2003. p. 3 v(xxvii, 1504, 1598 p.).
27. Zeimet AG, Marth C, Offner FA, Obrist P, Uhl-Steidl M, Feichtinger H, Stadlmann S, Daxenbichler G, Dapunt O. Human peritoneal mesothelial cells are more potent than ovarian cancer cells in producing tumor marker CA-125. *Gynecol Oncol*. 1996; 62:384–389. [PubMed: 8812537]
28. Helzlsouer KJ, Bush TL, Alberg AJ, Bass KM, Zacur H, Comstock GW. Prospective study of serum CA-125 levels as markers of ovarian cancer. *JAMA*. 1993; 269:1123–1126. [PubMed: 8433467]
29. Nossov V, Amneus M, Su F, Lang J, Janco JM, Reddy ST, Farias-Eisner R. The early detection of ovarian cancer: from traditional methods to proteomics. Can we really do better than serum CA-125? *Am J Obstet Gynecol*. 2008; 199:215–223. [PubMed: 18468571]
30. Alcazar JL, Guerriero S, Laparte C, Ajossa S, Jurado M. Contribution of power Doppler blood flow mapping to gray-scale ultrasound for predicting malignancy of adnexal masses in symptomatic and asymptomatic women. *Eur J Obstet Gynecol Reprod Biol*. 2011
31. D'Souza AL, Tseng JR, Pauly KB, Guccione S, Rosenberg J, Gambhir SS, Glazer GM. A strategy for blood biomarker amplification and localization using ultrasound. *Proc Natl Acad Sci U S A*. 2009; 106:17152–17157. [PubMed: 19805109]
32. Gaster RS, Hall DA, Nielsen CH, Osterfeld SJ, Yu H, Mach KE, Wilson RJ, Murmann B, Liao JC, Gambhir SS, Wang SX. Matrix-insensitive protein assays push the limits of biosensors in medicine. *Nat Med*. 2009; 15:1327–1332. [PubMed: 19820717]
33. Fishbein I, Levy RJ. Analytical chemistry: The matrix neutralized. *Nature*. 2009; 461:890–891. [PubMed: 19829362]
34. Almog N. Molecular mechanisms underlying tumor dormancy. *Cancer Lett*. 2010; 294:139–146. [PubMed: 20363069]
35. Goss PE, Chambers AF. Does tumour dormancy offer a therapeutic target? *Nat Rev Cancer*. 2010; 10:871–877. [PubMed: 21048784]
36. Jones S, Chen WD, Parmigiani G, Diehl F, Beerewinkel N, Antal T, Traulsen A, Nowak MA, Siegel C, Velculescu VE, Kinzler KW, Vogelstein B, Willis J, Markowitz SD. Comparative lesion sequencing provides insights into tumor evolution. *Proc Natl Acad Sci U S A*. 2008; 105:4283–4288. [PubMed: 18337506]
37. Luebeck EG. Cancer: Genomic evolution of metastasis. *Nature*. 2010; 467:1053–1055. [PubMed: 20981088]
38. Yachida S, Jones S, Bozic I, Antal T, Leary R, Fu B, Kamiyama M, Hruban RH, Eshleman JR, Nowak MA, Velculescu VE, Kinzler KW, Vogelstein B, Jacobuzio-Donahue CA. Distant metastasis occurs late during the genetic evolution of pancreatic cancer. *Nature*. 2010; 467:1114–1117. [PubMed: 20981102]
39. Meza R, Jeon J, Moolgavkar SH, Luebeck EG. Age-specific incidence of cancer: Phases, transitions, and biological implications. *Proc Natl Acad Sci U S A*. 2008; 105:16284–16289. [PubMed: 18936480]
40. Krebs HB, Goplerud DR, Kilpatrick SJ, Myers MB, Hunt A. Role of Ca 125 as tumor marker in ovarian carcinoma. *Obstet Gynecol*. 1986; 67:473–477. [PubMed: 3008052]
41. Lavin PT, Knapp RC, Malkasian G, Whitney CW, Berek JC, Bast RC Jr. CA 125 for the monitoring of ovarian carcinoma during primary therapy. *Obstet Gynecol*. 1987; 69:223–227. [PubMed: 2433652]

42. Hawkins RE, Roberts K, Wiltshaw E, Mundy J, McCready VR. The clinical correlates of serum CA125 in 169 patients with epithelial ovarian carcinoma. *Br J Cancer*. 1989; 60:634–637. [PubMed: 2803938]
43. Knapp, RC.; Berkowitz, RS. *Gynecologic oncology*. ed. 2nd. New York: McGraw-Hill, Health Professions Division; 1993. pp. xi, 500 p.
44. Jain RK, Munn LL, Fukumura D. Dissecting tumour pathophysiology using intravital microscopy. *Nat Rev Cancer*. 2002; 2:266–276. [PubMed: 12001988]
45. Teng CY, Wu TY. Secretory fluorescent protein, a secretion green fluorescent fusion protein with alkaline phosphatase activity as a sensitive and traceable reporter in baculovirus expression system. *Biotechnol Lett*. 2007; 29:1019–1024. [PubMed: 17401545]
46. Hanash SM, Pitteri SJ, Faca VM. Mining the plasma proteome for cancer biomarkers. *Nature*. 2008; 452:571–579. [PubMed: 18385731]
47. Lu J, Getz G, Miska EA, Alvarez-Saavedra E, Lamb J, Peck D, Sweet-Cordero A, Ebert BL, Mak RH, Ferrando AA, Downing JR, Jacks T, Horvitz HR, Golub TR. MicroRNA expression profiles classify human cancers. *Nature*. 2005; 435:834–838. [PubMed: 15944708]

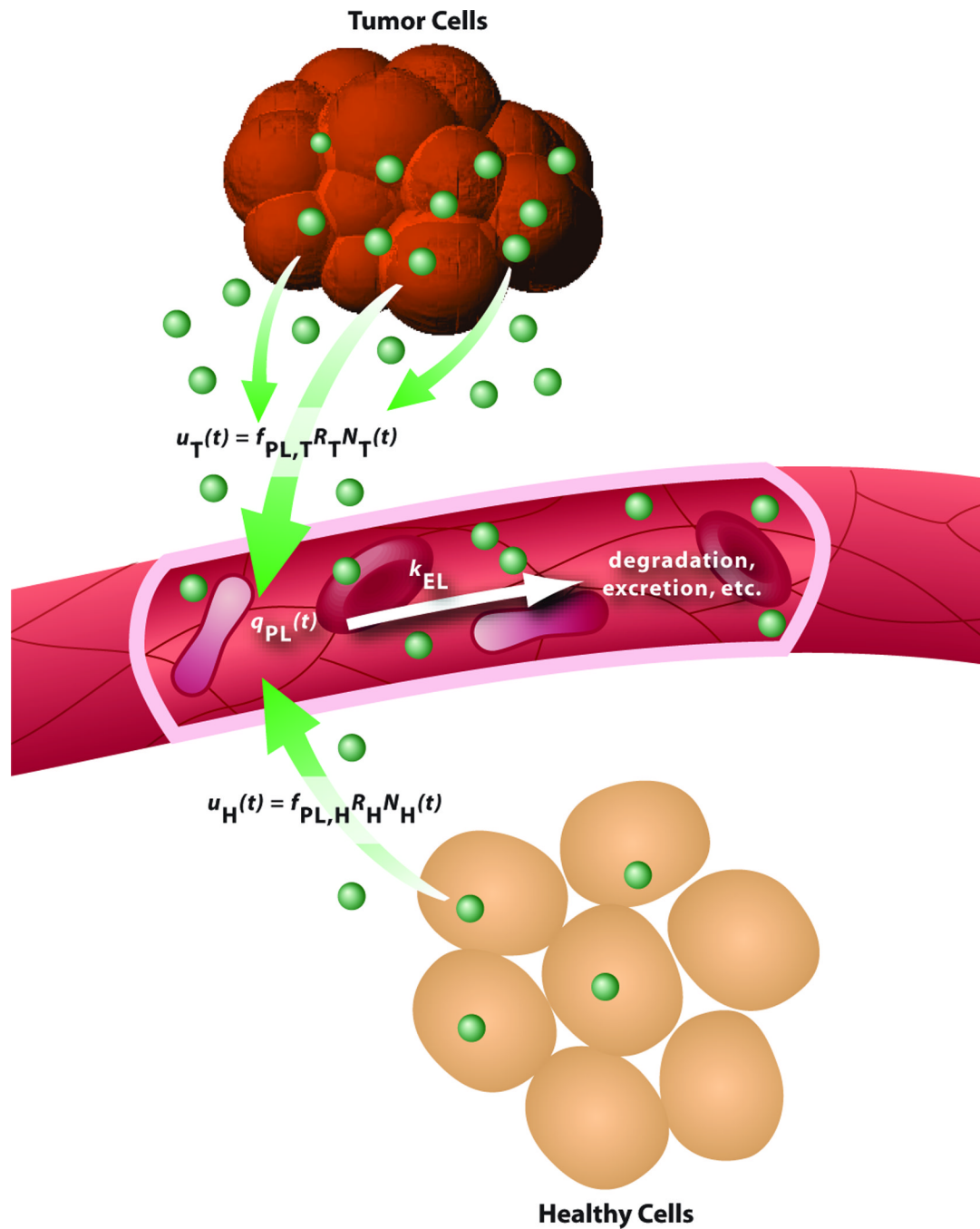


Fig. 1. One-compartment model for plasma biomarker kinetics

The change in the amount (mass) of plasma biomarker with respect to time is equal to the difference between the influx of biomarker into plasma, as shed by tumor cells and healthy cells, $u_T(t) + u_H(t)$, and the outflux of biomarker from plasma, $k_{EL}q_{PL}(t)$. See “Derivation of Model Equations” in the Supplementary Material.

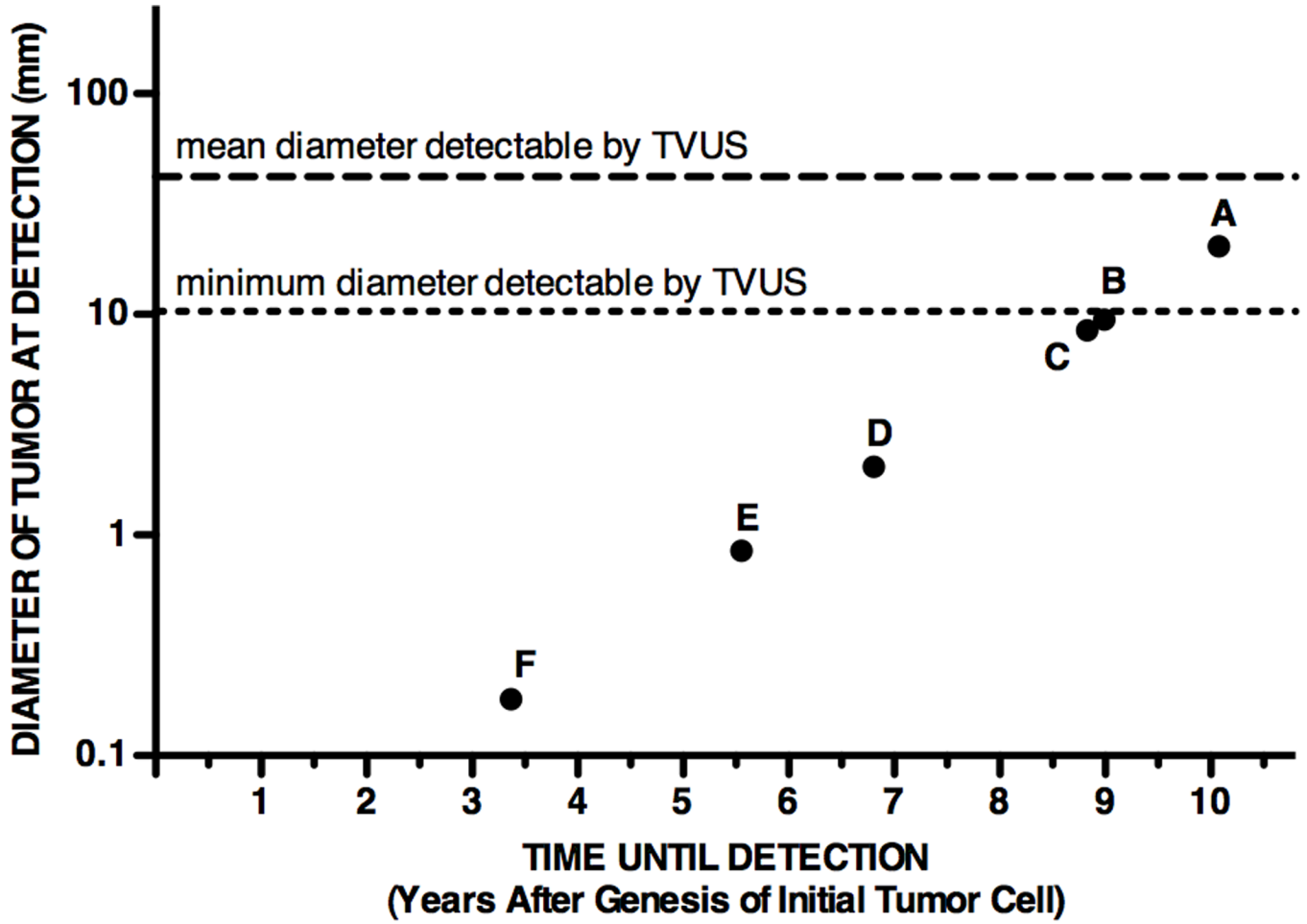


Fig. 2. Model-predicted detection capability of current and potential strategies for earlier cancer detection using blood biomarker assays
 See Table 2 for baseline parameter values. Dashed horizontal lines indicate the mean (42 mm) and minimum (10 mm) tumor diameters detected by transvaginal ultrasound (TVUS) in a study of 1,094 women with adnexal mass (30). Detection capability using: (A) current clinical ELISA assays (assuming baseline parameter values); (B) a biomarker that has 100% vascular permeability ($f_{PL,T} = 1$); (C) a biomarker not shed by healthy cells; (D) a biomarker shed by tumor cells at a rate 10^3 -fold higher than baseline; (E) a biomarker not shed by healthy cells, and decreasing assay detection limit 10^3 -fold relative to baseline; (F) a biomarker not shed by healthy cells, and decreasing assay detection limit 10^5 -fold relative to baseline.

Table 1
General Parameters for the Biomarker Shedding Model

Parameter values were based on ovarian carcinoma progression and CA125 shedding in the average female patient.

Parameter	Description (Units)	Fixed Value	Ref
V_{PL}	Mean plasma volume in a 70-kg female patient (ml)	3,150	(26)
q_{SS}/V_{PL}	Mean concentration of biomarker in healthy patient plasma (U/ml)	13.1	(22)
<i>density</i>	Expected tumor cell density in solid tumor (cells/mm ³)	1×10^6	(11, 19)
p	Percent of total tumor volume occupied by tumor cells	20	(11, 20)

Table 2
Biomarker Shedding and Tumor Growth Parameters Used in Sensitivity Analyses

Parameter values were based on ovarian carcinoma progression and CA125 shedding in the average female patient.

	Parameter	Description (Units)	Baseline Value	Range Simulated	Ref	
<i>Shedding by Tumor Cells Only</i>	$f_{PL,T}$	Fraction of biomarker entering tumor vasculature	0.1	1×10^{-4} to 1	–	
	R_T	Biomarker shedding rate per tumor cell (U/day/cell)	4.5×10^{-5}	4.5×10^{-11} to 0.45	(27)	
	$N_{T,0}$	Initial number of biomarker-shedding tumor cells	1	1 to 1×10^{10}	N/A	
	k_{GR}	Growth rate of tumor cell population (day^{-1})	5.78×10^{-3}	3.46×10^{-3} to 0.578	(18)	
	k_{EL}	Elimination rate of biomarker from plasma (day^{-1})	0.11	1.10×10^{-6} to 5.12	(23)	
	k_{cleasy}	Rate at which tumor growth rate decreases (day^{-1})	1×10^{-4}	1.29×10^{-6} to 2.15×10^{-4}	–	
	d	Detection limit of assay (U/ml)	1.5	1.5×10^{-9} to 15	(24, 25, 27)	
	<i>Shedding by Tumor and Healthy Cells</i>	$f_{PL,T}$	Fraction of biomarker entering tumor vasculature	0.1	1×10^{-4} to 1	–
		R_T	Biomarker shedding rate per tumor cell (U/day/cell)	4.5×10^{-5}	4.5×10^{-11} to 0.45	(27)
		$N_{T,0}$	Initial number of biomarker-shedding tumor cells	1	1 to 1×10^{10}	N/A
k_{GR}		Growth rate of tumor cell population (day^{-1})	5.78×10^{-3}	3.46×10^{-3} to 0.578	(18)	
k_{EL}		Elimination rate of biomarker from plasma (day^{-1})	0.11	1.10×10^{-6} to 5.12	(23)	
k_{cleasy}		Rate at which tumor growth rate decreases (day^{-1})	1×10^{-4}	1.29×10^{-6} to 2.15×10^{-4}	–	
$f_{PL,H} R_{HL} N_{H,0}$		Healthy cell shedding influx [†] (U/day)	4.56×10^3	4.56×10^{-6} to 4.56×10^4	(22)	
c		Plasma biomarker “cut-off” for healthy and disease states (U/ml)	34.11	13.6 to 75	(11, 17, 21)	

[†] Units of individual parameters are as follows: $f_{PL,H}$ (fraction), R_{HL} (U/day/cell) and $N_{H,0}$ (cells).

Table 3
Biomarker Shedding by Tumor Cells Only: Early Detection Times and Volumes for Baseline and Perturbed Parameter Values

Baseline conditions are shown in the first row and correspond to values in Table 2. Each cell in the model parameter category represents the value required to obtain the model-predicted values (tumor volume (mm³), diameter (mm) and detection time t_D (yr)) in the same row, with all other parameters remaining at their baseline values. For example, if $f_{PL,T}$ were changed to 1 from baseline value 0.1, a tumor of diameter 3.94 mm could be detected 7.7 years after its genesis. Values were calculated using the mono-exponential growth equation. Blank cells indicate that non-physiological parameter values (e.g., $f_{PL,T} > 1$, or $k_{EL} < 0$) would be required to achieve these model-predicted values.

Model-predicted values			Model parameter			
volume (mm ³)	diameter (mm)	t_D (yr)	$f_{PL,T}$ (fraction)	R_T (U/day/cell)	k_{EL} (day ⁻¹)	d (U/ml)
610	8.48	8.8	0.1	4.50×10^{-5}	1.10×10^{-1}	1.5
61	3.94	7.7	1	4.50×10^{-4}	5.84×10^{-3}	1.5×10^{-1}
6.1	1.83	6.7	–	4.50×10^{-3}	–	1.5×10^{-2}
0.61	0.85	5.6	–	4.50×10^{-2}	–	1.5×10^{-3}
0.061	0.39	4.5	–	4.50×10^{-1}	–	1.5×10^{-4}
6.1×10^{-3}	0.18	3.4	–	4.50×10^0	–	1.5×10^{-5}
6.1×10^{-4}	0.08	2.3	–	4.50×10^1	–	1.5×10^{-6}
6.1×10^{-5}	0.04	1.2	–	4.50×10^2	–	1.5×10^{-7}
6.1×10^{-6}	0.02	0.1	–	4.50×10^3	–	1.5×10^{-8}

Table 4
Biomarker Shedding by Tumor and Healthy Cells: Early Detection Times and Volumes for Baseline and Perturbed Parameter Values

Baseline conditions are shown in the first row and correspond to values in Table 2. Each cell in the model parameter category represents the value required to obtain the model-predicted values (tumor volume (mm^3), diameter (mm) and detection time t_D (yr)) in the same row, with all other parameters remaining at their baseline values. For example, if $f_{PL,T}$ were changed to 1 from baseline value 0.1, a tumor of diameter 9.49 mm could be detected 9.0 years after its genesis. Values were calculated using the mono-exponential growth equation. Blank cells indicate that non-physiological parameter values (e.g., $f_{PL,T} > 1$) would be required to achieve these model-predicted values.

Model-predicted values			Model parameter		
volume (mm^3)	diameter (mm)	t_D (yr)	$f_{PL,T}$ (fraction)	R_T (U/day/cell)	$f_{PL,T}R_HN_{H,0}$ (U/day)
8540	20.44	10.1	0.1	4.50×10^{-5}	4.56×10^3
854	9.49	9.0	1	4.50×10^{-4}	4.56×10^2
85.4	4.40	7.9	–	4.50×10^{-3}	4.56×10^1
8.54	2.04	6.8	–	4.50×10^{-2}	4.56×10^0
0.854	0.95	5.7	–	4.50×10^{-1}	4.56×10^{-1}
0.0854	0.44	4.6	–	4.50×10^0	4.56×10^{-2}
8.54×10^{-3}	0.20	3.5	–	4.50×10^1	4.56×10^{-3}
8.54×10^{-4}	0.09	2.4	–	4.50×10^2	4.56×10^{-4}
8.54×10^{-5}	0.04	1.4	–	4.50×10^3	4.56×10^{-5}